Demand Side Energy Management of EV Charging Stations by Approximate Dynamic Programming

Yu Wu[a,b*], Alexandre Ravey[a,b], Daniela Chrenko[a,b], Abdellatif Miraoui[ab]
[a]FEMTO-ST Institute, CNRS, Univ. Bourgogne Franche-Comte, UTBM, Belfort, France
[b]FCLAB, CNRS, Univ. Bourgogne Franche-Comte,UTBM, France
Email address: {yu.wu, alexandre.ravey, daniela.chrenko, abdellatif.miraoui}@utbm.fr

***Abstract*—The high operation cost of the EV charging station (EVCS) is a severe challenge for the development of electric vehicles, which lead to the general shortage of the EVCS. In order to reduce the operation costs of the EVCS, an approximate dynamic programming (ADP) based energy management system (EMS) is proposed for the EVCS equipped with multiple types of chargers (EVCS-MTC). A fuzzy logic guiding system has been designed to allocate each vehicle an appropriate charging spot based on its charging urgency. Multiple EVs can acquire the charging service through a common charger in the EVCS-MTC. In the proposed EMS, the approximate dynamic programming (ADP) and the evolution algorithm (EA) are combined to determine the optimal charging start time for each EV. This characteristic provides the charging device with the maximum autonomy to select the preferred flexible charging pattern, which can prolong the battery lifetime and reduce the communication requirements of the control system. With taking the dynamic electricity price and uncertain future charging demand into account, the proposed EMS can achieve a total cost reduction of over 50% compared with the conventional charging scheme in the numerical studies.**

Keywords: EV charging station; Demand side energy management; Approximate dynamic programming; flexible charging pattern; Multiple types of EV charger;

NOMENCLATURE

A. Indexes & abbreviation

i	index number for EV
j	index number for charger
L_i	charging laxity index of EV_i
ρ_i	normalized priority index of EV_i
S_j^v	charging speed capability index of charger j
M_j	demand index of charger j
EVCS	EV charging station
DP	dynamic programming
ADP	approximate dynamic programming
EMS	energy management system
BMS	battery management system of EV
SSC	single charger single cable system
MMC	multiple chargers multiple cables system
SMC	single charger multiple cables system (shared chargers)
UNC	uncoordinated immediate charging scheme
FL	fuzzy logic
EVCS-SSC	EV charging station with pure SSC
EVCS-MTC	EV charging station with multiple types of chargers (contains SSC and SMC)

B. Parameters

a_t	dynamic electricity price at time slot t (€/kWh)
a^p	penalty price of unsatisfied energy demand (€/kWh)
C_i^{ev}	battery capacity of EV_i (kWh)
N_i^{ev}	the allocated charger for EV_i
N^c	charger number of the EVCS
N_j^{cb}	cable number of charger j
n^{ev}	number of EVs at the charging station
n_t^c	the available charger number at time t
n^s	the capacity of the finite sets of Ω_{Ts}, Ω_{Ta} and Ω_{c_adp}.
n_j	number of the current EVs need to be charged at charger j
P^{ev}	average charging power of EV
$\widetilde{P_i}$	average power demand of EV_i over its parking time
$\widetilde{P_t^{cs}}$	average power demand of the EVCS at time t
SOC^f	final state of charge of the EV battery
SOC_i	initial SOC of EV_i
η	charging efficiency
γ	discount factor in ADP

C. *Variables*

x_i	charging start time of EV_i
Δx_i	estimated charging time of EV_i
H_j	scheduling horizon of charger j
C_j^{adp}	charging cost of charger j calculated by ADP
C_j	charging cost of current EVs at charger j
e_i^p	unsatisfied charging energy of EV_i (kWh)
$\widetilde{E_j^A}$	energy demand estimation of the charging station during horizon H_j
$\widetilde{e_j^a}$	energy demand estimation of charger j during the scheduling horizon H_j
S_t	charger state at time t
Ts_j	time range reserved for the current EVs at charger j
Ts_j^{min}	lower boundary of Ts
Ts_j^{max}	upper boundary of Ts
Ta_j	time range reserved for the future charging demand
t^c	the current time slot
t^A	the end time slot of the scheduling horizon H_j
t_i^{pk}	parking time of EV_i
t_i^{ar}	arrival time of EV_i
t_i^{dp}	departure time of EV_i
Δt	the decision time step
$\overline{V_j}$	approximation cost function of future charging demand at charger j
Ω_{c_adp}	the set of the discrete charging cost C_j^{adp} in ADP

1. Introduction

In the past decade, electrical vehicles (EV) have acquired vast attention as a promising solution to decrease the greenhouse gas emissions incurred by internal combustion engine (ICE) vehicles [1]. With the rapid development of battery technology and electrical powertrain technology, EVs are expected to play a dominant role in the future vehicle market. According to recent market reports of vehicle sales, EV sales around the world have maintained a growth rate of 42% since 2013[2]. In the meantime, the battery manufacturing costs have been reduced by 50% over the past 3 years [3]. However, the charging infrastructure is still a challenge to the expansion of the EV market. On one side, the shortage of charging facilities is an important factor that restrains the purchase interests of prospective customers. Those EV users without private chargers have to worry about the nearest EV charging facility. On the other side, the construction of tremendous charging facilities requires a large amount of investment costs and daily

maintenances [4-5]. Due to the large investments and blurred expected revenue, the present charging infrastructures are still far from enough [6-7]. Thus, more EV charging stations (EVCSs) are still needed to provide charging services for the increasing number of EVs. Lots of research has been devoted to reducing the investments and daily operation costs through optimal planning [8-10] and energy management strategies [11-14].

The demand-side energy management strategies can be generally classified into two categories: 1) pricing approaches and 2) direct load control approaches. The pricing approaches aim to optimize the energy consumption of multiple demand-side consumers through time-variant electricity pricing. Specifically, the aggregators or EV owners can shift their load according to the announced electricity price mechanism designed by the utility grid, and the total load curves can then be regulated accordingly [15-16]. However, the pricing strategies usually heavily rely on the communication between the utility grid and the EV users. Another challenge is the acceptance level of the designed dynamic electricity prices for EV users, who are supposed to cooperate with the time-variant dynamic price signals. This certainly requires self-discipline from the EV users. Meanwhile, the direct load control strategies coordinate the energy consumption by directly modulating the EV charging power. Many studies have been conducted with the aim of reducing the operation costs and satisfying the charging demand of EV users.

Linear programming is a widely used optimization technique for the scheduling problem of EV charging. In [17], an linear programming based charging scheme was proposed to minimize the total charging cost of EVs, while a fuzzy linear programming based bidding scheme was used in [18] to maximize the ancillary service revenue of EV aggregators. In [19], Xu et al. proposed a hierarchical control strategy for multiple EV aggregators in a time of use (TOU) price market. Here, linear programming was used to minimize the total electricity cost and reduce the power peak, and then the charging power of each EV was decided by a heuristic algorithm.

As an extension of linear programming, a mixed integer linear programming model was developed for the charging and reserve scheduling of an EV parking lot with renewable generations in [20-21], while a

day-ahead bidding and scheduling of EV fleets was proposed in [22]. In order to deal with the uncertainties of EV behaviors, and the electricity price market, some stochastic linear programming based models were developed in [23-24]. However, this kind of stochastic linear programming models depend on sufficient application scenarios to improve the optimization precisions, which significantly increases the computation burden and limits their applications. Furthermore, in order to achieve a faster charging speed and maintain a constant charging power for the EV batteries, in [25] Yao et al. proposed a binary optimization model to obtain a near-optimal on-off charging strategy in which the linear programming based model was solved through a convex relaxation method. Here, the on-off charging of EV batteries was enabled, since it was suggested in [26, 27] that constant charging power can prolong the batteries' service time and achieve a faster charging rate. Quadratic programming (QP) was used to minimize the overall load variance in a regional micro-grid in [28], while a decentralized charging protocol based on QP was used to achieve the valley filling for the grid operators in [29]. A real time energy management of EV charging station equipped with local generations was proposed in [30], where the energy gap between EV power demand and the local generations was minimized through QP.

To obtain more flexibility in the control strategies (multiple platform support, solving some non-linear formulations), some heuristic optimization models were investigated in studies [31-33]. In [32], a heuristic charging strategy for commercial buildings containing photovoltaic (PV) and EV system was proposed, where the EV charging rate was adjusted according to the variation of PV generation and the charging priority of each EV. Similarly, in [33], a centralized heuristic charging strategy was proposed to achieve the valley-filling for large-scale EVs. Meanwhile, some meta-heuristic based optimization methods were investigated in [34-38]. Particle swarm optimization (PSO) is used to minimize the power grid cost and maximize the EV users' satisfactions in [34], while a PSO-based EMS was developed to determine the optimal charging power in [35]. In [36], a Monte Carlo simulation based PSO was used to optimize the V2G capacities of EVs. In [37], a two-layer evolution strategy PSO was developed to reduce the power peak and provide frequency regulation services. Elsewhere, a game-theoretic based framework was designed for

multiple agents of EVs, in which the PSO technique was used to reach the game equilibrium [38]. However, while the heuristic control strategies have the advantages of more flexibilities and easier implementation, they are generally designed for specific applications, and thus their versatility has been weakened to some extent. Dynamic programming (DP) is notable for its global optimality, despite the rapidly growing computation burden with the number of system state variables. In [39], a DP optimization method was proposed for the EV fleet charging, where the computation burden was reduced through the designed aggregate battery model. In [40], a bi-level optimization framework was proposed for an EV fleet, where the inner loop calculated the optimal charging power based on DP, and the outer loop utilized a multi-objective GA to decide the final SOC. In order to effectively relieve the high computation issue of the conventional DP, approximate dynamic programming (ADP) was developed to overcome the "dimension curse" issue of DP, and the system uncertainties can be also addressed through the approximation modelling [41]. In [42], a two-stage ADP framework based charging strategy was proposed to determine the optimal charging energy amount for each EV at each time slot. Elsewhere in [43], an ADP based home energy management system was proposed to achieve the optimal scheduling and the demand response of the house energy consumption and the local PV generations.

Although many of the previous studies successfully managed the charging scheduling problem incorporating different scenarios, an important fundamental issue still arises from the deficiency of EV chargers versus the rapidly growing number of EVs. However, the aforementioned studies generally assumed that the installed EV chargers would be sufficient for the incoming EVs, and the proposed EV charging scheduling strategies were designed for the single charger single cable charging spot (SSC). In this paper, the authors have developed an ADP based EV charging strategy for the intelligent parking lots with multiple types of EV chargers, including the SSC and the shared chargers (i.e. single charger with multiple cables, SMC [44-45]). Compared to the widely used single charger single cable charging spot (SSC), the shared charger includes one charger with multiple cables which can be accessed by multiple EVs. From the view of investment efficiency, shared chargers have a higher utilization rate and lower initial investment

cost, which can make them advantageous to install in official or residential parking lots. In [46-47], mixed integer linear programming based EMSs were investigated for the parking lots equipped with shared chargers and PV panels, where two shared chargers with six EVs were studied. However, the limited scalability and the interruptible charging process could become barriers to their engineering application.

Another aspect that is seldom mentioned in the related existing research is the charging autonomy at the device level. Specifically, a constant power charging pattern was suggested to prolong the batteries' lifetime in [25-27], whereas in [48, 49], the charging current was designed as a function of cycle number to maximize the lifetime of lithium battery. In [50], a varying current decay charging pattern was developed to obtain a faster charging speed and lower capacity fades of lithium batteries. In [51], a multi-objective optimization approach was developed to obtain the feasible charging pattern with considering the temperature variations. Though different charging patterns were developed to enhance the battery performance and the lifetime in the abovementioned studies, the common point is that they all require the charging autonomy at the device level [52]. This means that it is preferable that the instantaneous charging power of EV is determined by the battery management system (BMS) of EVs (or the local charging device) rather than the upper level EMS. However, most of the direct load control strategies introduced in the aforementioned studies require controlling the charging rates or the on/off charging states of each EV directly, which could not guarantee the charging autonomy at the device level.

In this work, an ADP based EMS is developed for the EV charging station with multiple types of chargers (EVCS-MTC). The constraints of shared chargers and the stochastic nature of EV behaviors will be also considered. The proposed EMS only determines the optimal charging start time of each EV rather than controlling the on-off charging states or the charging rates. This characteristic provides the maximum charging autonomy at the device level. One obvious advantage over some other studies is that, it can avoid the significant fade of battery capacity due to the intermittent charging/discharging process [53]. Another merit of this strategy is that, it appears more practical to be implemented in smart charging applications, where the instructions of the charging power amount are generally obtained from the BMS of EV (or the

local charging device) instead of the charging station [54]. Moreover, since only the charging start signal is required during the charging process, the communication burden of the control system can be vastly reduced.

This paper is organized as follows. Section II introduces the EV charging station equipped with multiple types of charges (EVCS-MTC). Section III introduces the overall energy management system (EMS) framework and the designed fuzzy logic guiding system. In Section IV, a myopic charging scheme is developed to deal with the optimal scheduling of current EVs, and then the ADP-based EMS is proposed to obtain the global optimal charging policy in consideration of the future charging demand. Finally, in Section V, numerical case studies of the EVCS in residential and workplace parking lots are conducted. The uncoordinated immediate charging scheme is used as the benchmark to prove the effectiveness of the proposed EMS. Besides, comparative studies between the EVCS with pure SSC systems (EVCS-SSC) and the EVCS-MTC are conducted. In Section V, the conclusions of this paper are drawn, as well.

2. EV Charging Stations with Multiple Types of Chargers

Different types of charging facilities are reviewed in this section, including the single charger single cable system (SSC), the multiple charger multiple cables system (MMC), and the single charger multiple cables system (SMC), as shown in Figure 1. Then, the scheduling problem of the EVCS-MTC is presented.

2.1. Comparison of Different Types of Charging Spots

An EV charger is usually comprised of three parts: a power converter, a cable, and a socket-outlet. Among these components, the power converter is the most expensive, due to its complicated structure and numerous semiconductor devices [4]. Generally, three types of charging systems can be found in the EV parking lots, including the single charger single cable system (SSC), the multiple chargers multiple cables system (MMC), and the single charger multiple cables system (SMC), as shown in Fig 1. The SSC system is designed to charge an EV individually, whereas the MMC system can charge several EVs simultaneously. Since the MMC utilizes multiple power converters and cables to achieve multiple EV charging (Fig.1b), it can be regarded as a combination of several SSC. Thus, their investment costs are approximately the same. Different from the SSC or the MMC, the SMC achieves multiple EV charging through a single power converter and

multiple cables (Fig.1c), which means that multiple EVs can share one power converter during their parking time in sequence [44-45].

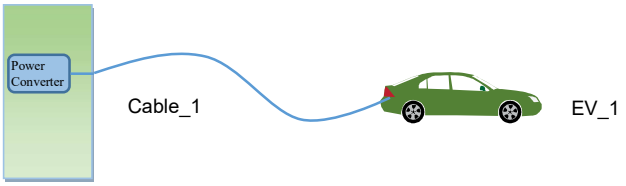

(a) Single charger with single cable (SSC)

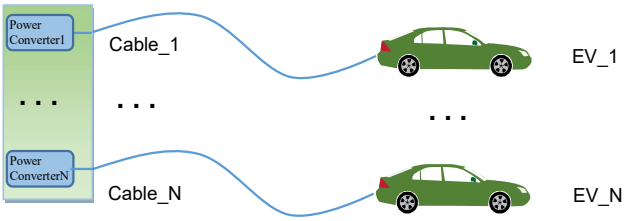

(b) Multiple chargers with multiple cables (MMC)

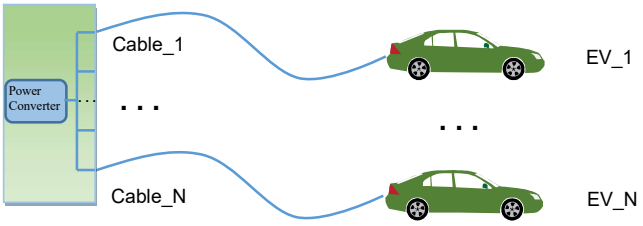

(c) Single charger with multiple cables (SMC, shared chargers)

Fig. 1. Different types of charging spots

2.2. Problem Statement

In this paper, the authors consider an EV charging station incorporating both SSC and SMC, which is suitable to be installed near residential communities or work sites. The EVs with relative short parking time can be charged at SSC, while the EVs with relative long parking time can be charged at SMC.

While the SMC system (the shared charging spot) takes the advantage of low initial investment, it suffers from the issue of charging time conflict [44]. When multiple EVs share one charger in sequence, the total charging time can occasionally exceed the total parking time. This will lead to inevitable charging time conflicts. The operation cost of an EVCS can be formulated as follows:

$$Cost(\boldsymbol{x_i}) = \sum_{i=1}^{n^{ev}} \sum_{t=x_i}^{x_i+\Delta x_i} P^{ev} \cdot a_t \cdot \Delta t + \sum_{i=1}^{n^{ev}} e_i^p(x_i) \cdot a^p \quad (1)$$

$$\Delta x_i \approx \frac{(SOC^f - SOC_i) \cdot C_i^{ev}}{\eta \cdot P^{ev}} \quad (2)$$

where x_i is the charging start time of EV_i, n^{ev} is the total EV number, Δx_i is the estimated charging time of EV_i, a_t is the real time electricity price, $e_i^p(x_i)$ is the unsatisfied energy of EV_i, a^p is the penalty price of the unsatisfied energy demand. SOC^f is the target SOC value set by the EV owner, SOC_i is the initial SOC value of EV_i, C_i^{ev} is the EV battery capacity, P^{ev} is the average charging power of EV, η is the charging efficiency. Here, the average charging power P^{ev} is used to estimate the required charging time, while the real time charging power pattern is decided by the EV battery management system (BMS) or the local charging device. Thus, the following aspects are considered in the formulated scheduling problem of EV charging: 1) The physical constraints of EV chargers (e.g. multiple EVs share an SMC in sequence). 2) Continuous charging process of each EV (to ensure the charging pattern autonomy at the device level). 3) Minimizing the total operation cost of the EVCS.

3. System Framework

3.1. Overview of the Energy Management System

In order to reduce the operation costs of the EV charging station, an ADP based energy management system is proposed for the EVCS-MTC, as shown in Fig.2. Firstly, a fuzzy logic based guiding system has been designed to allocate the EV to its specific charging spot. With the designed fuzzy logic controller, each EV can be coordinately allocated to the corresponding charging spot according to its urgency levels. Secondly, after connecting to the corresponding charger, the EV will be controlled to charge from the optimal start time based on the designed EMS.

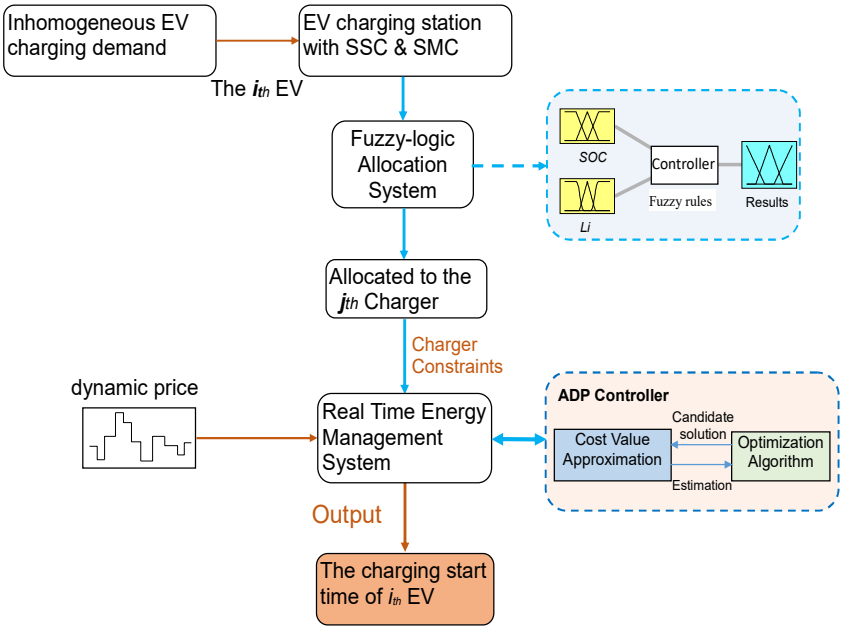

Fig. 2. The proposed control system of EV charging stations

3.2. Fuzzy Logic Allocation System

The charging station has different types of charging spots, while the EVs have different levels of charging urgencies (different parking time and charging demand). In this section, a fuzzy logic based guiding system has been designed to lead the EV to the appropriate charging spot. Firstly, the authors design a laxity index L_i to represent the charging urgencies of different EVs in (3):

$$L_i = \frac{t_i^{pk} - \Delta x_i}{\Delta x_i} \ , \ t_i^{pk} = t_i^{dp} - t_i^{ar} \tag{3}$$

where t_i^{pk} is the parking time of EV_i, t_i^{dp} is the departure time, and t_i^{ar} is the arrival time EV_i. The laxity index L_i is defined as the ratio of the estimated charging time Δx_i and the "laxity time" $(t_i^{pk} - \Delta x_i)$. The larger value of L_i means that the EV_i has more flexibility to be controlled by the EMS.

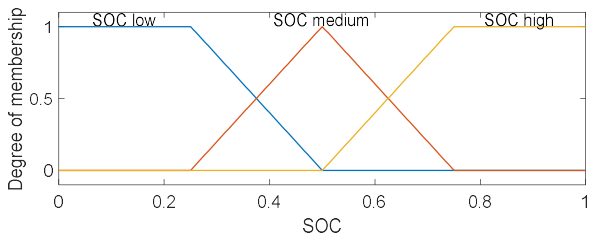

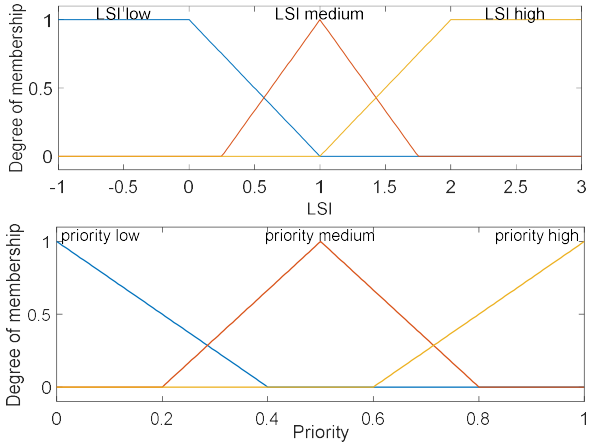

Fig. 3. Membership functions of fuzzy logic controller

TABLE I. Fuzzy Rules of Charging Priority

***L* (laxity)**	**SOC**	**Charging priority**
L	L,M,H	H
M	L,M,H	M
H	L,M	M
H	H	L

The membership functions of laxity index L_i, SOC, and the charging priority index are defined in Figure.3, where the membership functions of each variable are classified into three groups (L, M, and H) respectively. The corresponding fuzzy rules are depicted in Table I. With the designed fuzzy logic controller, the priority index ρ_i of EV_i can be obtained accordingly, which has been finally normalized to [0, 1]. Further, in order to evaluate the charging speed capability of different chargers in a quantitative way, a speed index S_j^v is defined in (4~5). The index has a negative correlation with the cable number N_j^{cb} and the charging demand index M_j.

$$S_j^v = \frac{1 + e^{-M_j}}{N_j^{cb}} \tag{4}$$

$$M_j = \sum_{i=1}^{n} \frac{\Delta x_i}{t_i^{pk}} \tag{5}$$

where the S_j^v is the charging speed index of the charger j, N_j^{cb} is the cable number of j_{th} charger, M_j is the demand index which is used to represent the current charging demand amount. The defined index S_j^v ensures that, an EV charger with fewer cables and less charging demand will have a higher value of S_j^v.

$$\Omega_{ch} = \{charger[1], \dots, charger[n_t^c]\} \quad (6)$$

$$N_i^{ev} = [\rho_i \cdot n_t^c] \quad (7)$$

Finally, all the available chargers can be ranked from small to large according to the index S_j^v, forming a set Ω_{ch} of quantity n_t^c in (6). The new EV arrival will be allocated to the $N_i^{ev}th$ charging spot (7). The allocation process is illustrated with details in **Algorithm 1**.

Algorithm 1 Fuzzy-logic Allocation Algorithm

Step 1. Detecting new EV arrivals

1a. Collect information of new EV arrivals, record the SOC state and calculate the laxity index according to (3).

Step 2. Obtain the priority index of each EV

2a. Input the laxity value L_i and the battery status SOC_i of EV_i into the fuzzy logic controller.

2b. Obtain the priority index value ρ_i of EV_i from the fuzzy logic controller.

Step 3. Collect information of the available chargers with idle cables. Rank all the chargers based on speed index from small to large according to (4~6), and finally constitute the set Ω_{ch} of quantity n_t^c.

Step 4. Dispatch the new EV arrival to the corresponding charger. Specifically, the EV will be allocated to $[\rho_i * n_t^c]_{th}$ charger.

4. Optimal Charging Strategy

In this part, a myopic charging scheme is firstly designed to achieve the optimal economic charging with the information of current EVs. In order to decrease the time conflicts of SMC and take the future charging demand into account, an approximate dynamic programming (ADP) based charging scheme is further developed.

4.1. Myopic charging scheme

The myopic charging scheme is a kind of greedy strategy based on the current information, which is referred to the here-and-now decisions. In this scheme, the optimal charging start time of the EV depends on the lowest electricity price intervals within the scheduling horizon, neglecting the impact of these decisions on the future.

Specifically, the EVs are controlled to be charged during the lowest electricity price intervals with the corresponding constraints (8b~8d). A minimization problem is formulated for a single charging spot in formula (8a):

$$\min C_j(x_i) = \sum_{i}^{n_j} \sum_{t=x_i}^{x_i+\Delta x_i} P^{ev} \cdot a_t \cdot \Delta t \tag{8a}$$

$$\text{s.t.} \quad x_i \geq t_i^{ar}, \quad \forall i = 1 \dots n_j \tag{8b}$$

$$x_i + \Delta x_i \leq t_i^{dp}, \quad \forall i = 1 \dots n_j \tag{8c}$$

$$x_i + \Delta x_i \leq x_{i+1}, \quad \forall i = 1 \dots n_j - 1 \tag{8d}$$

where $C_j(x_i)$ is the cost function of charger j during the current scheduling horizon, x_i is the charging start time of EV_i, n_j is the current number of EVs need to be charged at charger j, t_i^{ar} is the arrival time of EV_i, t_i^{dp} is the departure time of EVi.

Formula (8b) ensures that the charging start time later than the EV arrival time, and formula (8c) ensures that the charging demand can be satisfied before the EV departure. The formula (8d) ensures that the charging process of each EV is continuous, and only one EV can be charged at the same time.

The authors note that the minimization problem (8a) is a typical nonlinear problem ($k \cdot C_j(x_i) \neq C_j(k \cdot x_i), k \in R^+$), thus the authors adopted a hybrid evolution algorithm to solve it [55], as shown in **Fig.4**. In Figure.4, the initial population is the random feasible solution of the charging start time for the EVs at charger j, M is the iteration number, N is the parent population number. The fitness value is calculated through the cost function in (8a).

Regarding the charging time conflict issue of the shared charging spot, the problem (8a) is firstly checked for its feasibility according to the constraints (8b~8d) in the algorithm flowchart (Figure.4). If the constraints are satisfied, the hybrid evolution algorithm can output the optimal charging start time vector $\boldsymbol{x}$ for the EVs after iterations. The EVs at the same charger spot follow the earliest deadline first charging

principle [56]. The earliest departure EV will be charged firstly according to the obtained results $\boldsymbol{x}$. On the contrary, if the charging time conflict occurs, which means the constraints (8b~8d) are not satisfied, the EVs will be charged immediately to avoid further penalties.

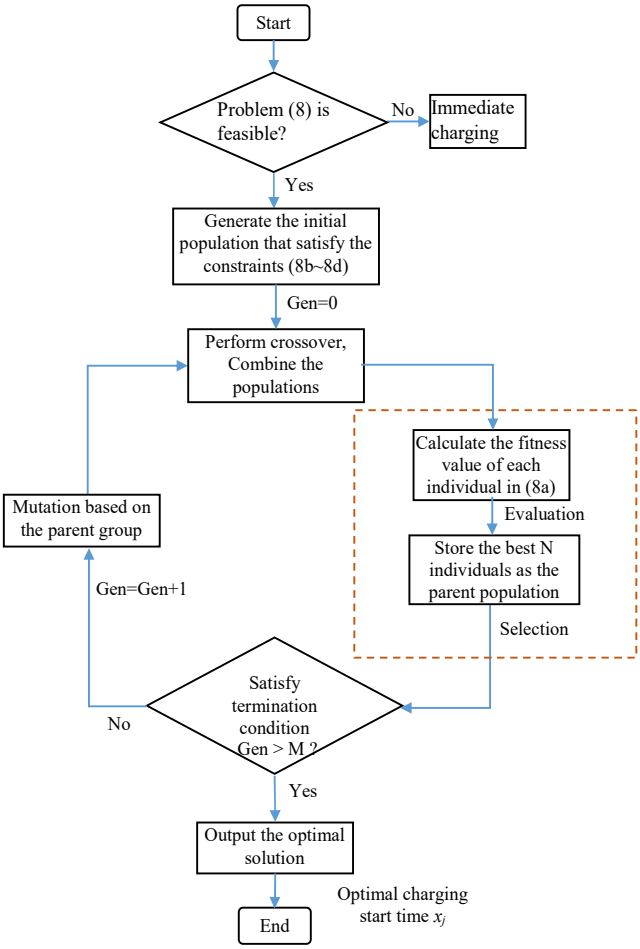

Fig. 4. The hybrid evolution algorithm (**Algorithm 2**)

4.2. Approximate Dynamic Programming

Since the myopic optimal strategy only involves the information of current EVs, it cannot provide a global optimal policy. In this section, an approximate dynamic programming (ADP) framework combined with the EA algorithm is developed to solve the charging optimization problem of EVs. Considering the uncertain future charging demand, the global optimal charging policy can increase the charging demand satisfaction rate compared to the myopic policy.

A dynamic programming (DP) for the EV charging optimization problem can be formulated in a Bellman's optimality equation form:

$$V(S_t) = \min\left[C(S_t, x) + \gamma \sum_{s'} P(s'|S_t, x) \cdot V_{t+1}(s')\right] \tag{9}$$

where S_t represents the current charger state (the EV number, scheduling horizon, electricity price, etc.), V_t is the value function of state S_t, and γ is the discount factor. $C(S_t, x_t)$ is the reward if the action x_t is executed in state S_t , $P(s'|S_t, x_t)$ is the transition probability matrix, and s' is the next possible state after executing the action x. The optimal solution can be obtained by solving the Bellman optimality equation (9). However, finding an exact solution is computationally infeasible in most of the practical problems due to the massive dimensions of the state and action spaces [57]. The exact transition probability matrix of the system states is also difficult to define in the practical projects due to the lack of sufficient information. The approximate dynamic programming (ADP) provides an efficient solution to alleviate the computational bottleneck in DP by replacing the exact value function with an approximation of some sort of form. With the approximation of the value function, ADP can solve the optimization problem in a forward manner as opposed to the backward computations in DP. The optimal policy of ADP can be obtained as in formula (10):

$$X_t^* = arg\min_x \left[C(S_t, x) + \gamma \overline{V}(S_t, x)\right] \tag{10}$$

where $C(S_t,x)$ is the cost function of the current scheduling horizon, and $\overline{V}(S_t, x)$ is the approximate cost function of the future demand.

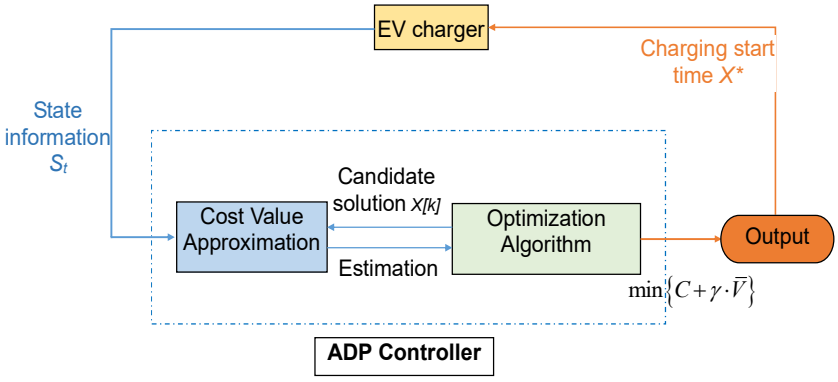

Fig. 5. The proposed ADP framework for the EV charging spot

The framework of the proposed ADP strategy is demonstrated in Figure.5. It is a program loop consisting of the cost value approximation and the optimization process. $\overline{V}(S_t, x)$ can be calculated through the cost approximation function, and $C(S_t, x)$ can be calculated through the optimization algorithm (Figure.4, Algorithm 2). Through the above calculation process, the optimal charging start time policy for the EV charging spot can be obtained.

From the perspective of the time line, the ADP process can be divided into two stages: the optimization stage, and the approximation stage (as shown in Figure.6). The optimization stage is similar to the myopic optimal policy presented in the previous section (Figure.4). It schedules the current charging demand optimally within the given time range Ts_j , while the time range Ta_j of the approximation stage is reserved for the future charging demand.

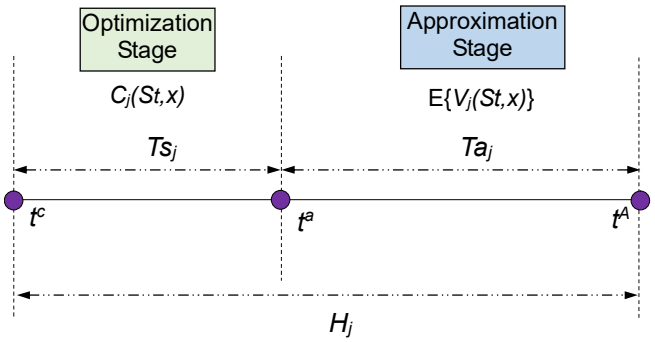

Fig. 6. the ADP process of an EV charger

In Figure.6, t^c is the current time slot, t^A is the end time slot of the scheduling horizon H_j, Ts_j is the time range reserved for the current charging demand, and Ta_j is the time range reserved for the future charging demand. H_j is the scheduling horizon of charger j, and it is equal to the longest parking time of the EV at charger j, as in formula (11).

$$H_j = max\left\{t_1^{pk}, \dots, t_{n_j}^{pk}\right\} \ , H_j = Ts_j + Ta_j \tag{11}$$

The lower boundary of Ts_j can be obtained by summing up each vehicle's charging demand time at charger j, and the upper boundary of Ts_j is equal to the horizon H_j, as demonstrated in formula (12).

$$Ts_j^{min} = \sum_{i}^{n_j} \Delta x_i \ , \ Ts_j^{max} = H_j \tag{12}$$

where Ts_j^{min} is the lower boundary of Ts_j. It is the minimum charging time to satisfy the current charging demand. The upper boundary Ts_j^{max} equals to the longest parking time of EV at charger j.

Since it is impossible to enumerate every possible value in the continuous set of Ts_j, a finite number of discrete Ts_j are evaluated here. With the boundaries of Ts_j and the decision time step Δt, the finite sets of Ts_j and Ta_j can be obtained in (13~14).

$$\Omega_{\mathrm{Ts}} = \{Ts_j[1], \dots, Ts_j[n^s]\}, \qquad n^s = \frac{Ts_j^{max} - Ts_j^{min}}{\Delta t} \tag{13}$$

$$\Omega_{\mathrm{Ta}} = \{Ta_j[1], \dots, Ta_j[n^s]\}, \qquad Ta_j[n^s] = H_j - Ts_j[n^s] \tag{14}$$

Thus, the total cost C_j^{adp} of ADP can be obtained by summing up the costs of the optimization stage and the approximation stage:

$$C_j^{adp}(S_t) = C_j\big(S_t(Ts_j), x\big) + \gamma \overline{V_j}\big(S_t(Ta_j)\big) \tag{15}$$

For each state S_t of charger j, there is a corresponding total cost C_j^{adp}. $\Omega_{\text{c-adp}}$ is used to denote the set of all the possible cost C_j^{adp}.

$$\Omega_{c\_adp} = \{C_j^{adp}[1], \dots, C_j^{adp}[n^s]\} \tag{16}$$

In the solution set of $\Omega_{\text{c-adp}}$, the global optimal cost and the corresponding optimal policy X_j^* can be found in (17).

$$C_j^{adp*} = min\{\Omega_{c\_adp}\}, \qquad X_j^* = arg\ \min_x\{\Omega_{c\_adp}\} \tag{17}$$

1) Optimization Stage

In the optimization stage, the cost C_j of charger j in (15) can be obtained by solving the following problem with **Algorithm 2** (Figure.4):

$$\min C_j(S_t(Ts_j), x) = \sum_{i}^{n_j} \sum_{t=x_i}^{x_i+\Delta x_i} P^{ev} \cdot a_t \cdot \Delta t \tag{18a}$$

$$\text{s.t.} \qquad x_i \geq t_i^{ar}\,, \qquad \forall i = 1 \ldots n_j \tag{18b}$$

$$x_i + \Delta x_i \leq t_i^{dp}\,, \qquad \forall i = 1 \ldots n_j \tag{18c}$$

$$x_i + \Delta x_i \leq x_{i+1}\,, \quad \forall i = 1 \ldots (n_j - 1) \tag{18d}$$

$$x_i + \Delta x_i \leq t^c + Ts_j\,, \qquad \forall i = 1 \ldots n_j \tag{18e}$$

Here, the optimization process is similar to the myopic optimal strategy with an extra constraint (18e). The constraint (18e) ensures that the charging demands of current EVs can be satisfied within the time range Ts_j. Thus, the hybrid EA designed in the previous section is used to solve it.

2) Approximation stage

In the approximation stage, the approximated value function $\overline{V_j}$ is necessary to be well designed to avoid the dimensionality issue of DP. For the vehicle parking lots in the work sites and residential communities, the statistics of vehicle staying patterns follow the time-dependent distributions. A fixed parametric model appears to have difficulty specifying and characterizing all day's charging demand, while the simulation based methods are well adapted to reveal the dependency between the future charging demand and the electricity cost [42]. Thus, in this study, a Monte Carlo simulation based nonparametric cost function is developed to approximate the future charging demand at different time intervals over one day.

Firstly, the average power demand $\widetilde{P_i}$ of a single EV over its parking time can be calculated in formula (19). Similarly, for the charging station at time slot *t*, the power demand density can be obtained through calculating formula (20).

$$\widetilde{P_i} = \frac{\Delta x_i \cdot P^{ev}}{t_i^{pk}} \tag{19}$$

$$\widetilde{P_t^{cs}} = \sum_{i}^{n_t^{ev}} \widetilde{P_i} \tag{20}$$

where n_t^{ev} is the number of the current vehicles parked in the charging station. For a period of time H_j, the demand estimation of the charging station can be formulated in (21). Thus, the demand estimation of charger j during its scheduling horizon H_j can be approximately obtained with formulas (21~23). The future charging demand of charger j can be divided into two parts: the satisfied demand $\widetilde{e_j^s}$, and the unsatisfied part $\widetilde{e_j^p}$. In (23), $\Delta x'$ is the charging duration time of the satisfied part, x' is the virtual charging start time of the future charging demand, and t^A is the end time slot of H_j (Fig.6).

$$\widetilde{E_j^A} = \sum_{t}^{t+H_j} \widetilde{P_t^{cs}} \cdot \Delta t \tag{21}$$

$$\widetilde{e_j^a} = \frac{\widetilde{E_j^A}}{N^c} = \widetilde{e_j^s} + \widetilde{e_j^p} \tag{22}$$

$$\Delta x' = t^A - x' = \frac{\widetilde{e_j^s}}{P^{ev}} \tag{23}$$

Then the approximated cost function in (24a) can be obtained by summing up the electricity costs and the penalty costs.

$$\overline{V_j} = \min E\left\{ \sum_{t=x'}^{x'+\Delta x'} a_t \cdot P^{ev} \cdot \Delta t + \widetilde{e_j^p} \cdot a^p \right\} \tag{24a}$$

$$S.t. \qquad t^c + Ts_j \le x' \le t^c + H_j \tag{24b}$$

$$\widetilde{e_j^p} = \widetilde{e_j^a} - \widetilde{e_j^s} = \widetilde{e_j^a} - P^{ev} \cdot \Delta x' \tag{24c}$$

The value space of x' is limited in (24b), thus the value function (24a) can be effectively solved by line search methods [29]. Consequently, with the optimization stage cost $C_j(S_t,x)$ in (18a) and the approximated future cost $\overline{V_j}$ in (24a), the global optimal policy can be obtained through formula (17). To demonstrate the ADP charging scheme clearly, the flowchart is presented in Figure.7, and the pseudo code of the ADP is briefly presented in **Algorithm 3**.

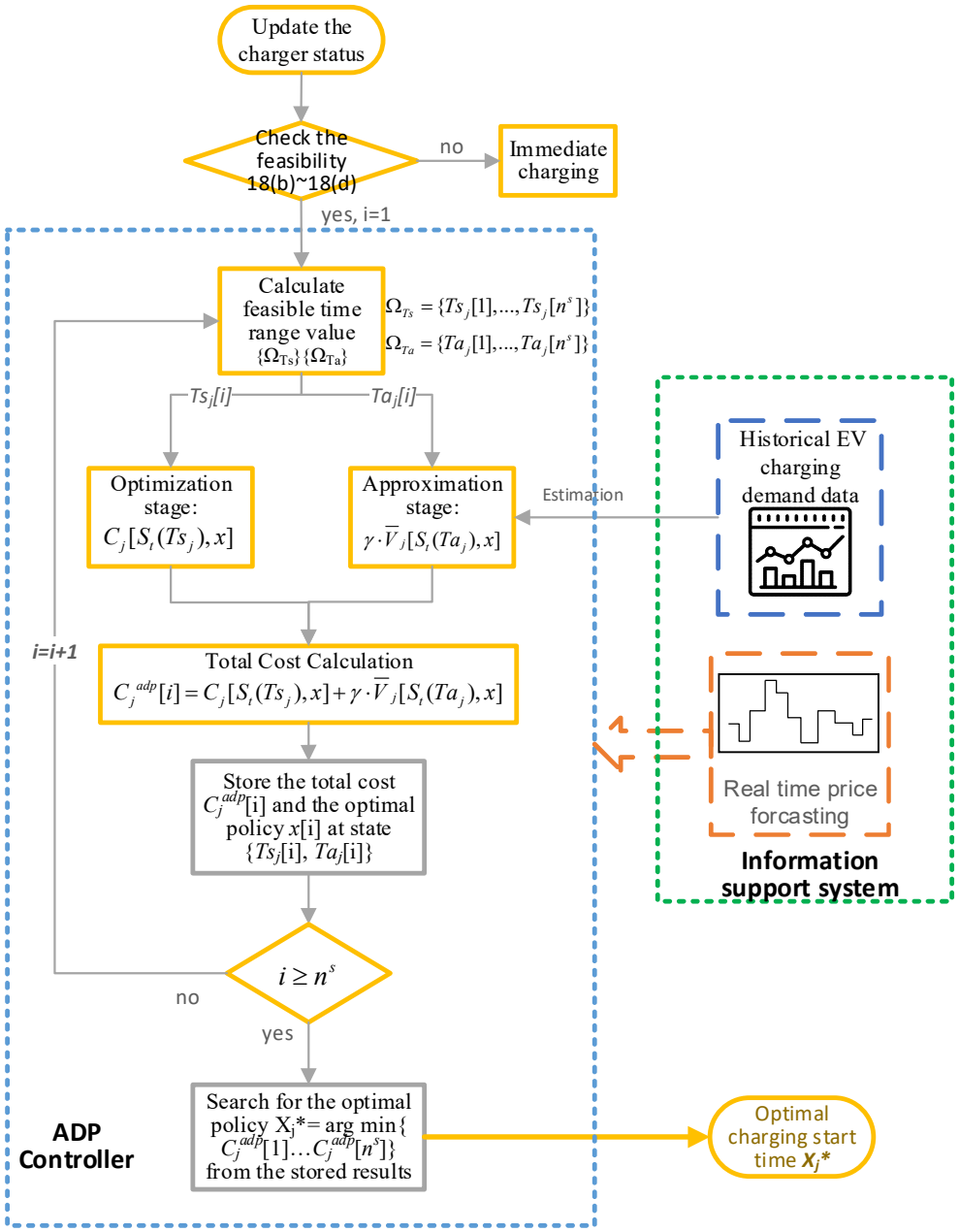

Fig. 7. The flowchart of the ADP charging scheme

Algorithm 3 Approximate Dynamic Programming

Step 1. Fuzzy logic allocation of EV arrivals

1a. Evaluate the charging priorities of new arriving EVs

1b. Rank the available charging spots according to the speed index

1c. Allocate the EV to the corresponding charging spot

Step 2. Initialization of ADP

2a. update the status of charger j (EV number, initial SOC, arrival time, departure time)

2b. Collect the predictions of the dynamic electricity price

Step 3. Optimization and approximation of ADP

3a. Calculate the feasible time range of optimization stage: Ts (Ω_{Ts} $=\{Ts[1],..., Ts[k],...Ts[n^s]\}$), obtain the state set of charger j: S_t(Ts) $=\{S_t(Ts[1]),..., S_t(Ts[k],..., S_t(Ts[n^s]\}$.

3b. For each state $S_t(Ts[k])$ **do** :

3c. (Optimization stage) **Go to Algorithm 2.** Calculate the minimal cost $C_j(S_t,x)$ in (18) and obtain the corresponding policy $x_j[k]$.

3d. (Approximation stage) Calculate the future approximate cost $\bar{V}[S_t, x']$ with formula (24).

3e. Calculate the total cost $C_j^{adp}[k]$ according to formula (15) with the minimal cost $C_j(S_t,x)$ from 3c, and the approximate future cost $\bar{V}_j[S_t, x']$ from 3d.

3f. Store the total cost $C_j^{adp}[k]$ and the corresponding policy $x_j[k]$ at state $S_t(Ts[k])$.

3g. $k=k+1$. **If** $k>n^s$, **End for.**

Step 4. Policy evaluation and execution

4a. Search for the optimal policy $x_j^*= \arg\min\{ C_j^{adp}[1],..., C_j^{adp}[k] \ldots C_j^{adp}[n^s]\}$ from the stored results in Step 3f.

4b. Execute the policy x_j^*, and update the status of charger j and the EVs.

4c. Set $t_c=t_c+1$, **go to** step 1.

4.3. Benchmark charging schemes

The uncoordinated immediate charging scheme (UNC) is used as the benchmark in this paper, because it is widely applied in current EVCSs. With this charging scheme, the EV user randomly selects an EV charging spot for charging, and the EV can be charged immediately if the charging spot is available. The immediate charging scheme has also been combined with the fuzzy logic guiding system to verify the improvement of the charger utilization rate. Moreover, the comparative studies between the EVCS with pure SSC systems (EVCS-SSC) and the EVCS-MTC are conducted to highlight the advantages of the proposed ADP-based EMS.

5. Case Study

5.1. Case overview and parameter settings

The simulations are implemented in a real time horrizon-rolling maner. The future EV arrivals are unkown at the current decision time slot. The case studies of this paper will be based on the residential and the official parking lots, where the parking pattern generally follows a time-varying distribution. (e.g. the residential parking lots have a high arrival rate in the evening and a high departure rate in the morning). Since the Poisson distribution is well adapted for traffic flow analysis, the vehicle arrival distribution is modeled as a Poisson process based on the historical data in the National Household Travel Survey (NHTS) 2009 [58].

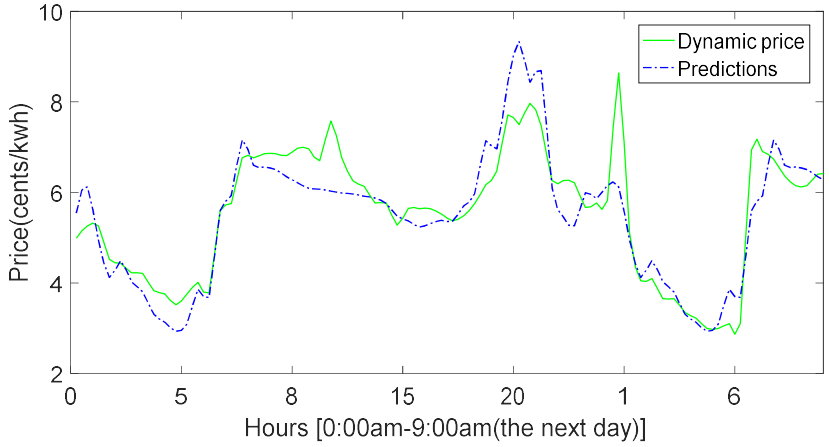

Fig. 8. Electricity price prediction of Oct.19, 2017

The dynamic electricity price market of France is used as the price signal here [59]. A classical ARMA forecasting method is adopted to predict the electricity price [60], and the prediction results are shown in Figure.8 (unit: cents €/kWh). As the authors focus on the energy management of EV charging in this paper, the details of electricity price forecasting are not introduced here. Some electricity markets can also provide a price forecasting service or a day-ahead price, such as ComEd, ERCOT day-ahead market [45, 61]. In order to reduce the unsatisfied energy demand, the penalty price is set as 15 cents €/kWh, about 3 times of the normal price.

TABLE II. Charger Settings of EVCS-MTC and EVCS-SSC

EV Charging Station Type	**Settings of Cable**	**Charger Type**				**Total spot number**
		SSC	***SMC(a)***	***SMC(b)***	***SMC(c)***	
	Cable quantity	1	2	3	4	
EVCS-MTC	Charger quantity	5	5	20	10	115
EVCS-SSC	Charger quantity	115	0	0	0	115

In the EMS, the decision time step Δt is 15 min, the iteration number M of EA is 50, the parent population number N of EA is 30, and the discount factor γ of ADP is 0.8. The charging efficiency η is 0.9. The average charging power P^{ev} is 8kW, which belongs to a Level 2 charging station [4]. The battery capacity of EV is assumed to be 50kWh, and the final target SOC of EV is set as 100%. The vehicle capacity of the parking lots is set as 115 vehicles, which allows maximum 115 EVs to be charged. Specifically, the settings of the two types of EVCS are shown in Table II, where there are total 40 chargers with 115 cables in the EV

charging station equipped with multiple chargers (EVCS-MTC) and 115 chargers in the EV charging stations equipped with SSC (EVCS-SSC).

5.2. Application scenario A (residential parking lots)

In this section, numerical case studies with 143 EVs in a residential parking lot are conducted. The EV arrivals are divided into two groups: the arrivals during the daytime (between 9.am and 4.pm) are assumed to be the short stays, and the arrivals after 4.pm are assumed to be long stays for overnight charging. The parking time of the short stays is assumed to follow a Gaussian distribution $N(3\text{h},0.5\text{h}^2)$. The departure time of the long stay EVs are assumed to follow a Gaussian distribution $N(8{:}00\ \text{a.m},1\text{h}^2)$. Their initial SOC are assumed to follow the Gaussian distributions (i.e. $SOC_i \sim N(0.7,\ 0.08^2)$ for the short stay charging, $SOC_i \sim N(0.4,0.15^2)$ for the overnight charging). The vehicle stay pattern of the residential parking lots is shown in Figure.9.

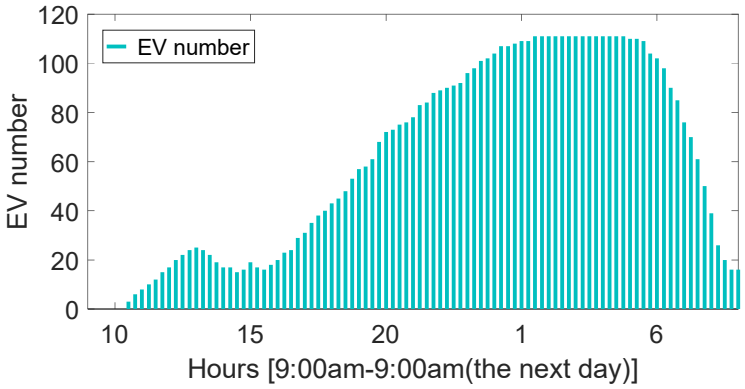

Fig. 9. EV number in the residential parking lot (EV stay pattern)

1) The simulation results and analysis of ADP controlled EVCS-MTC(Case A1)

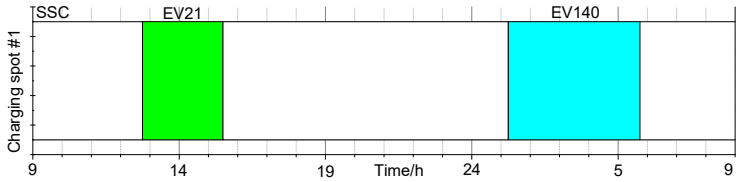

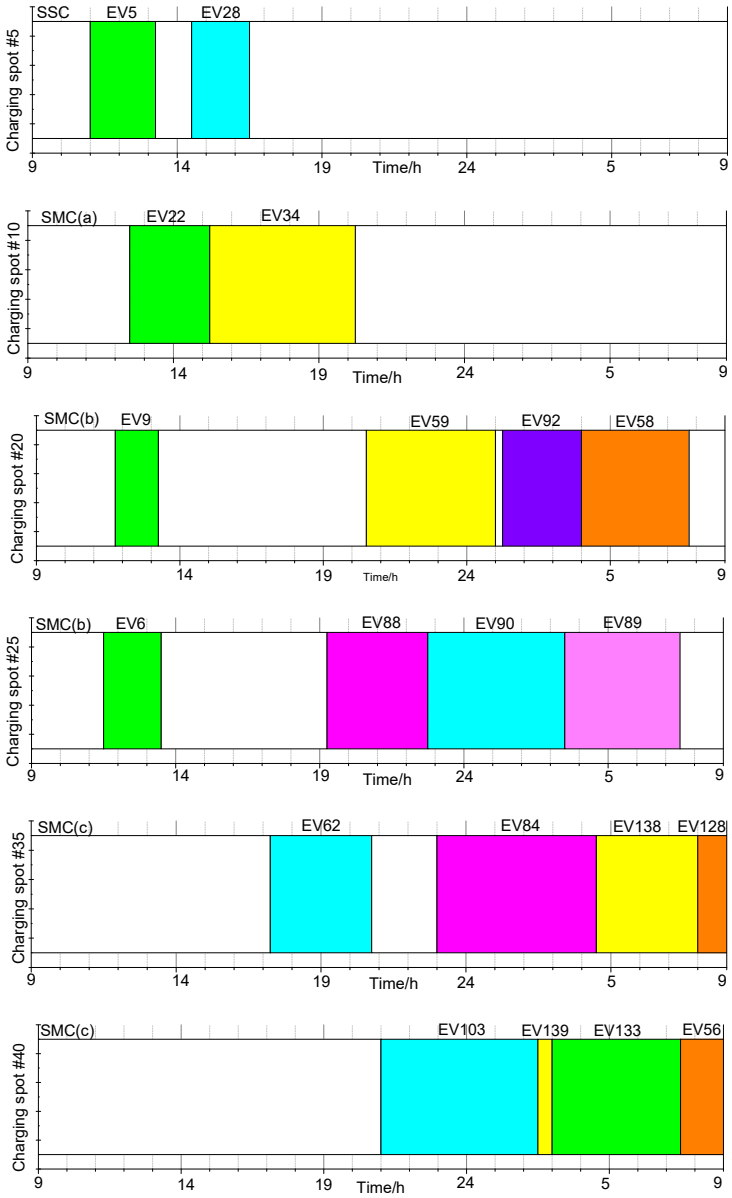

Fig. 10. Operation profiles of charger #1, #5, #10, #20, #25, #35, #40.

In Figure.10, the operation profiles of different chargers in EVCS-MTC are presented (controlled by FL-ADP). It is clear that multiple EVs can share one SMC system, and the SMC system has a higher utilization rate than the SSC system. With its single charging cable, the SSC system provides charging services for less EVs.

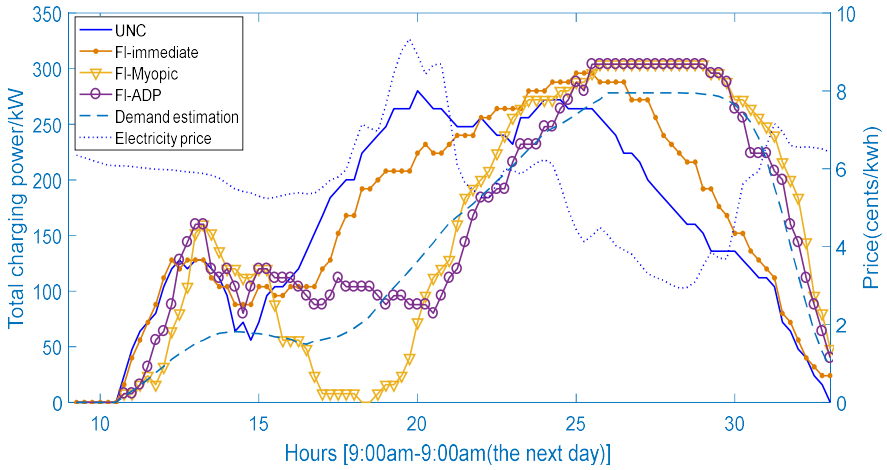

Fig. 11. Total charging power profile in case A1

The total charging power profiles of different charging schemes are shown in Figure.11. The bechmark scheme, i.e. the uncoordinated immediate charging scheme (UNC) always charges the vehicles without delay, as shown by the blue line in Figure.11. The myopic charging scheme always charges the current vhehicle in the lowest price interval, as shown by the yellow line. Lastly, the fuzzy logic ADP charging scheme charges the vehicles in consideration of both the electricity price and the uncertain future charging demand, as shown by the purple-circle line.

In the ADP charging scheme, the future energy demand can be approximately estimated by the designed demand estimation model, and the estimation results are shown by the dashed lines in Figure.11. It can be observed that the proposed estimation model matches the real demand value well. In the meantime, the demand estimation values can be updated with the historical charging data to improve its precision.

TABLE III. Charging Costs of Case A1

Charging Schemes	**Charging Costs(€)**			
	Electricity costs	***Penalty***	***Satisfied energy (%)***	***Costs/€***
UNC	216.42	33.90	94.40	250.32
FL-IMC	217.10	10.50	98.27	227.60
FL-Myopic	189.87	39.60	93.46	229.47
FL-ADP	198.66	18.90	96.88	217.56

The charging costs of the different charging schemes in Case A are listed in Table III. Since the uncoordinated immediate charging (UNC) and fuzzy logic-immediate charging (FL-IMC) satisfy the EVs as soon as possible, their electricity costs are higher than the other two charging schemes. On the other side, the FL-myopic charging scheme always charges the EV during the lowest electricity price intervals, so its electricity costs are the lowest among the charging schemes. However, due to its negligence of future charging demand, the myopic charging scheme has a relatively high penalty cost caused by the unsatisfied energy. Thus, the FL-ADP charging scheme displays a balanced performance over the other charging schemes (lower electricity costs than the immediate charging schemes, lower penalty costs than the myopic charging scheme), and has the lowest total charging costs.

Meanwhile, in Table III, it is clear that FL-IMC has a higher satisfied energy rate than the UNC scheme. With the designed fuzzy logic controller, the EVs can be coordinately dispatched to their proper charging spots, which could help reduce the unsatisfied charging demand.

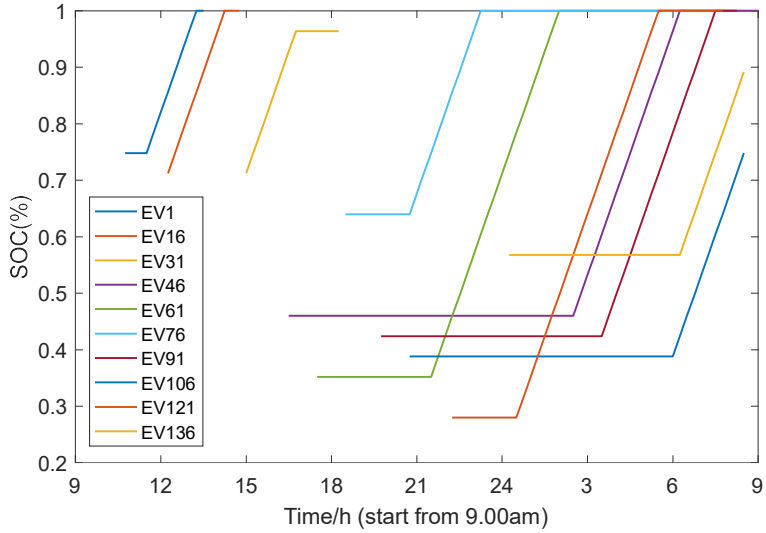

Fig. 12. Charging profiles of EVs in Case A with ADP control

In Figure.12, the charging profiles of 10 EVs are clearly illustrated. It can be seen that the charging process of each EV is continuous. Therefore, the obtained uninterruptible charging process can provide the BMS (or the local charging device) with the maximum autonomy to select the preferred flexible charging pattern, which can be used to prolong the battery lifetime or accelerate the EV charging.

2) Comparative study between the EVCS-SSC and the EVCS-MTC controlled by ADP(Case A2)

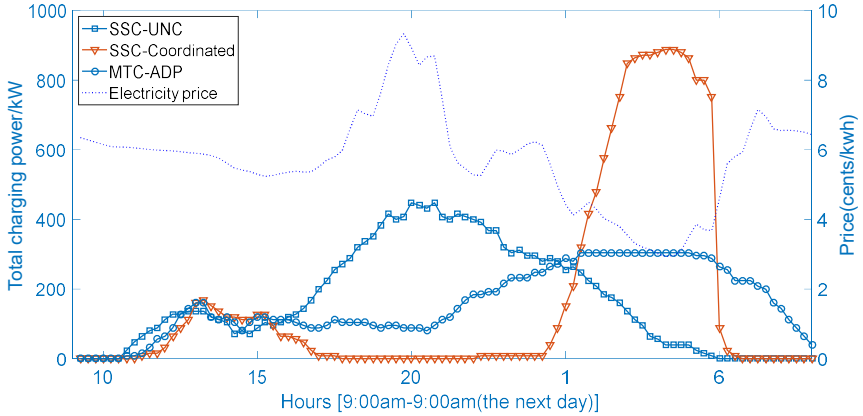

Fig. 13. Charging power comparisions between the EVCS-SSC and the EVCS-MTC in Case A2

Since the EVCS-SSC is widely applied at present, a comparative study between the EVCS-SSC (only contains SSC) and the EVCS-MTC (contains SSC and SMC) is conducted. The same 143 EVs' profiles are used here (arrival time, departure time, SOC, etc.). The total charging power profiles are presented in Figure.13, in which the coordinated charging in EVCS-SSC is shown by the orange line, the uncoordinated immediate charging is shown by the blue-square line, and the ADP charging with EVCS-MTC is shown by the purple-circle line.

The daily total costs comparison has been calculated in Table IV, including the electricity consumption costs, daily investment costs, and the unsatisfied energy penalties. Here, the hardware cost of each charging spot is 4000€, and the maintenance and repair cost rate is 400€/year (about 10% of the material cost) [62]. The service life of each charging spot is assumed to be 15 years [62, 63]. The extra cable cost for the SMC is set as 50€/per cable (the material cost is about 5 €/m), and the cost of a load switch is assumed to be 20€ [44]. For simplicity, the installation costs of the chargers are neglected here. The material costs and the maintenance costs are necessary for the daily operation of an EVCS, which are calculated as the daily investment item in Table IV.

In Table IV, it is clear that the electricity costs of the coordinated SSC charging scheme are the lowest. However, the power peak load of the coordinated SSC charging scheme is much higher than that of the other

schemes, which could be another concern for the local grid operator. Besides, it is also clear that the daily total costs of the proposed ADP charging scheme is the lowest. A cost reduction of about 56% can be achieved compared to the uncoordinated SSC charging.

TABLE IV. Cost Comparisons of the EVCS-SSC and the EVCS-MTC Controlled by ADP

Spot Type	Control strategy	Spot number	Power peak (kW)	Daily Investment (€)	Electricity costs (€)	Penalty (€)	Satisfied energy (%)	Daily total costs(€)
SSC	Uncoordinated	115	476	210.05	245.68	0	100	455.73
SSC	Coordinated	115	887	210.05	148.15	0	100	358.20
MTC	ADP	40	310	74.16	198.66	18.90	96.88	291.72

5.3. Application scenario B (office building parking lots)

In this section, the optimal charging schemes of the EVCS-MTC in an office building district is studied. Similar to the previous section, the EV arrival is modeled as a Poisson process. The departure time of EVs is assumed to follow a Gaussian distribution $N(18{:}00, 1\text{hour}^2)$. The total number of EV is 119, and the vehicle stay pattern of the office district is presented in Figure.14.

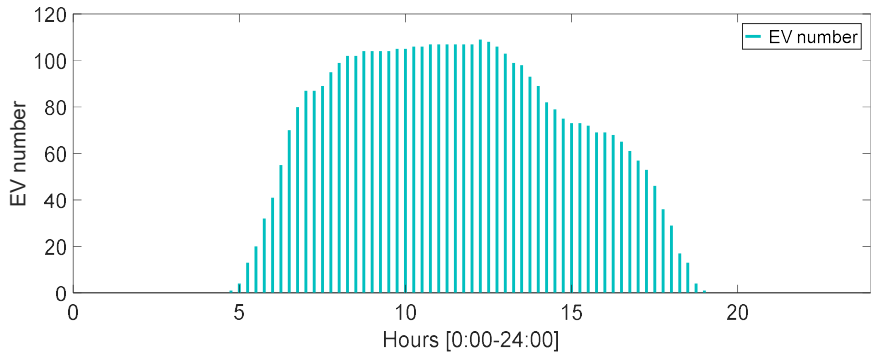

Fig. 14. EV number in office building parking lot(vehicle stay pattern)

1) The simulation results and analysis of ADP controlled EVCS-MTC (Case B1)

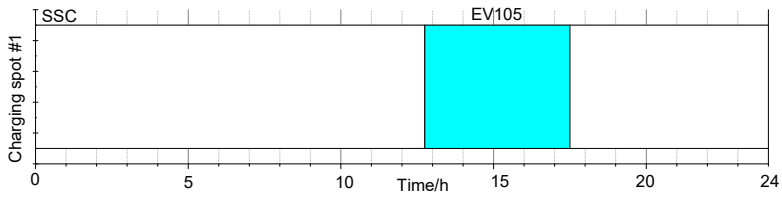

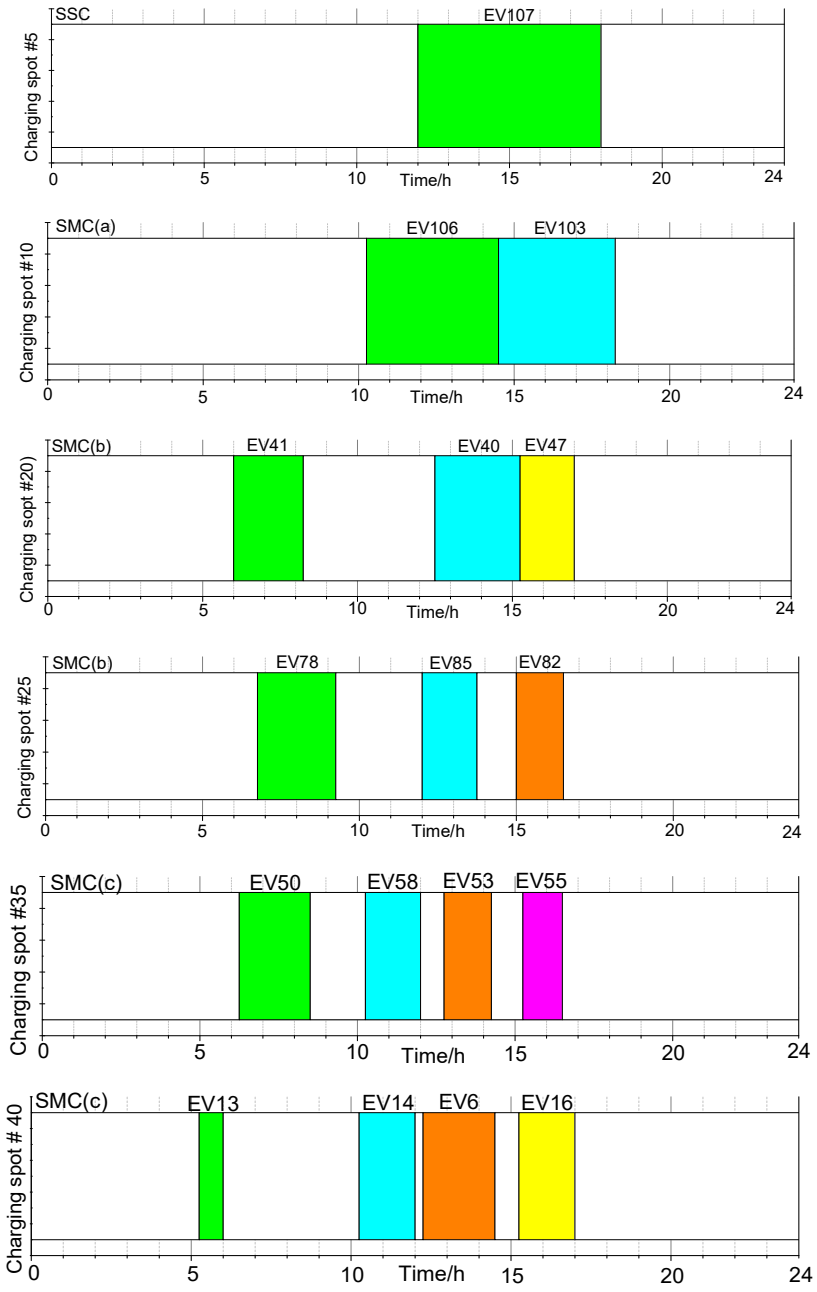

Fig. 15. Operation profiles of EV charger #1, #5, #10, #20, #25, #35, #40.

As show in Figure.15, the operation profiles of EVCS-MTC are presented. It is clear that the SMC has a higher utilization rate than the SSC. With the designed the fuzzy guiding system, the EVs are coordinately dispatched to the corresponding charging spot. More EVs can be charged through the multi-cables of the SMC, while the “urgent” EVs can be charged at SSC.

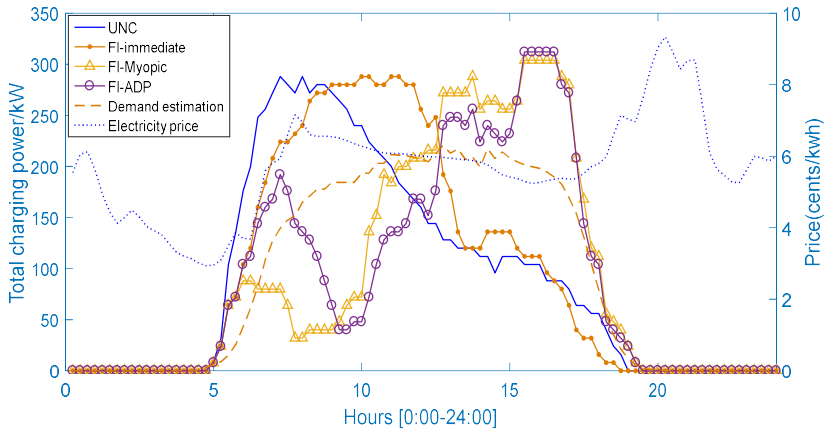

Fig. 16. Total charging power profile in case B1

In Figure.16, the charging load profiles are presented. It can be observed that the immediate charging schemes charge the EVs without any delay, while the myopic and the ADP charging scheme charge the EVs during the low price intervals. With the limited charger number of the EVCS-MTC, the peak power of the charging schemes are similar. The charging costs are listed in Table V. Similar to the previous section, the immediate charging schemes (UNC and FL-IMC) have higher electricity costs. Without the designed fuzzy logic guiding system, the penalty costs of UNC scheme are the highest. This illustrates the effectiveness of the designed guiding system. Meanwhile, considering both the dynamic price and the future charging demand, the proposed ADP charging scheme has the lowest charging costs.

TABLE V. Charging Costs of Case B1

Charging Schemes	**Charging Costs(€)**			
	Electricity costs	***Penalty***	***Satisfied energy (%)***	***Costs/ €***
UNC	134.58	15.60	95.45	150.18
FL-IMC	144.75	0.60	99.83	145.35
FL-Myopic	132.85	8.40	97.55	141.25
FL-ADP	132.06	8.10	97.64	140.16

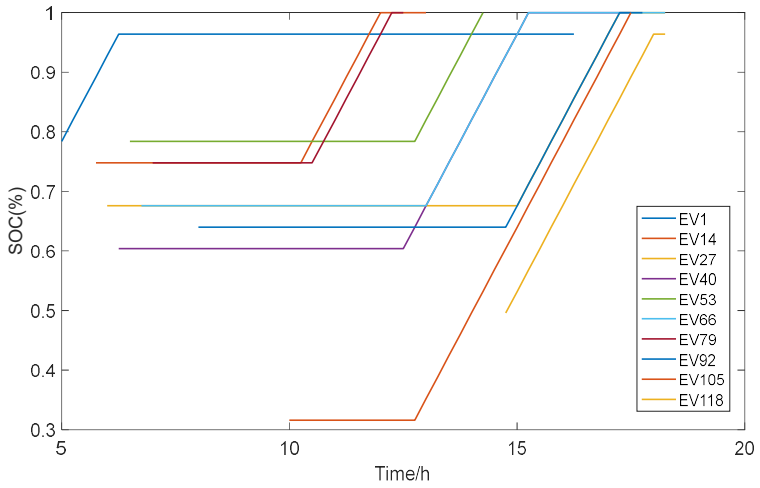

Fig. 17. Charging profiles of EVs in Case B with ADP control

The charging profiles of 10 EVs are presented in Figure.17. It can be observed that the charging process of each EV is uninterruptible. This characteristic gives the BMS (or the local charger) the maximum autonomy to define the preferred charging pattern to prolong the battery lifetime or accelerate the charging speed.

2) Comparative study between the EVCS-SSC and the EVCS-MTC controlled by ADP (Case B2)

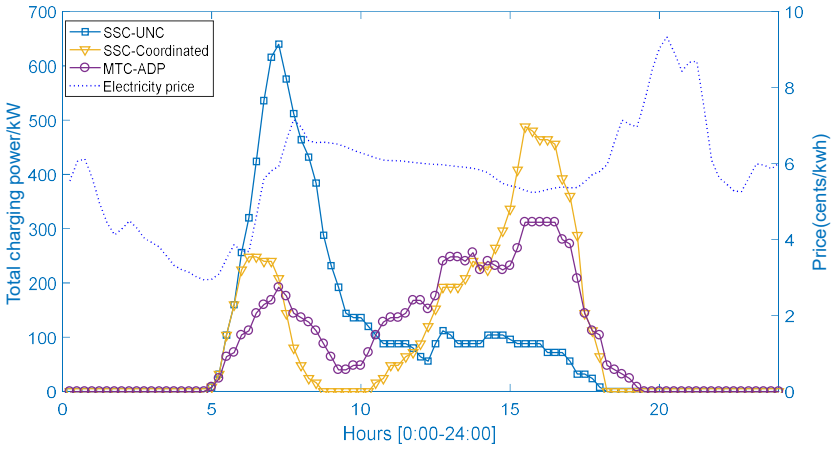

Fig. 18. Charging power comparisions between the EVCS-SSC and the EVCS-MTC in Case B2

With the same 119 EVs' profiles in the office building parking lot, a comparative study between the EVCS-SSC and the EVCS-MTC is conducted. The total charging load are presented in Figure.18. It is clear that the immediate charging scheme with EVCS-SSC could lead to the highest peak power in this case. With

the corresponding hardware material costs and the maintenance costs, the total operation costs are calculated in Table VI. Similar to the previous section, the installation costs are neglected here. Although the electricity costs of the coordinated charging with EVCS-SSC are lower than the proposed ADP charging scheme, the induced peak load power is much higher. Besides, it is clear that the daily costs of ADP are the lowest among the charging schemes. A cost reduction of about 61.90% can be achieved compared to the uncoordinated charging scheme.

TABLE VI. Cost Comparisons of the Uncoordinated SSC charging scheme and the ADP charging scheme

Spot Type	Control strategy	Spot number	Power peak (kW)	Daily investment (€)	Electricity costs (€)	Penalty (€)	Satisfied energy (%)	Daily total costs(€)
SSC	Uncoordinated	115	640	210.05	136.94	0	100	346.99
SSC	Coordinated	115	488	210.05	127.81	0	100	337.86
MTC	ADP	40	312	74.16	132.06	8.10	97.64	214.32

6. Conclusions

This paper explores the energy management strategies for the EV charging stations with multiple types of chargers (EVCS-MTC). An ADP based charging scheme is proposed for this type of EVCS, which determines the optimal charging start time of each EV in consideration of both the real time electricity price and uncertain future charging demand. A fuzzy logic guiding system is also designed to allocate the EVs to the proper charging spots according to their charging urgency levels. Compared to the related existing researches of energy management for EVCSs, the proposed energy management strategy is suitable for multiple types of charging spots (i.e. SSC and SMC). The operation costs can be reduced by over 50% compared to the immediate charging scheme in EVCS-SSC. Moreover, since only the charging start time of each EV is determined by the EMS, this provides the local charger (or the BMS) with the maximum autonomy to select the preferred flexible charging pattern to prolong the battery lifetime, and the communication burden of the control system can be reduced as well.

References

[1] N. S. Pearre and L. G. Swan, “Electric vehicle charging to support renewable energy integration in a capacity constrained electricity grid,” *Energy Convers. Manag.*, vol. 109, pp. 130–139, 2016.

[2] D. Hall, M. Moultak, and N. Lutsey, “Electric vehicle capitals of the world: Demonstrating the path to electric drive,” *Int. Counc. Clean Transp.*, no. March, p. 57, 2017.

[3] C. Curry, “Lithium-ion Battery Costs and Market,” *Bloom. New Energy Financ.*, p. 14, 2017.

[4] M. Yilmaz and P. T. Krein, “Review of battery charger topologies, charging power levels, and infrastructure for plug-in electric and hybrid vehicles,” *IEEE Trans. Power Electron.*, vol. 28, no. 5, pp. 2151–2169, 2013.

[5] L. Rubino, C. Capasso, and O. Veneri, “Review on plug-in electric vehicle charging architectures integrated with distributed energy sources for sustainable mobility,” *Appl. Energy*, 2017.

[6] C. Guo and C. C. Chan, “Analysis method and utilization mechanism of the overall value of EV charging,” *Energy Convers. Manag.*, vol. 89, pp. 420–426, 2015.

[7] R. Godina, E. M. G. Rodrigues, N. G. Paterakis, O. Erdinc, and J. P. S. Catalão, “Innovative impact assessment of electric vehicles charging loads on distribution transformers using real data,” *Energy Convers. Manag.*, vol. 120, pp. 206–216, 2016.

[8] D. Quoc, Z. Yang, and H. Trinh, “Determining the size of PHEV charging stations powered by commercial grid-integrated PV systems considering reactive power support,” *Appl. Energy*, vol. 183, pp. 160–169, 2016.

[9] H. Fathabadi, “Novel wind powered electric vehicle charging station with vehicle-to-grid (V2G) connection capability,” *Energy Convers. Manag.*, vol. 136, pp. 229–239, 2017.

[10] Y. Xiang, J. Liu, R. Li, F. Li, C. Gu, and S. Tang, “Economic planning of electric vehicle charging stations considering traffic constraints and load profile templates,” *Appl. Energy*, vol. 178, pp. 647–659, 2016.

[11] F. Fazelpour, M. Vafaeipour, O. Rahbari, and M. A. Rosen, “Intelligent optimization to integrate a plug-in hybrid electric vehicle smart parking lot with renewable energy resources and enhance grid characteristics,” *Energy Convers. Manag.*, vol. 77, pp. 250–261, 2014.

[12] A. El-Zonkoly, “Intelligent energy management of optimally located renewable energy systems incorporating PHEV,” *Energy Convers. Manag.*, vol. 84, pp. 427–435, 2014.

[13] M. Shafie-khah, M. P. Moghaddam, M. K. Sheikh-el-eslami, and J. P. S. Catalão, “Optimised performance of a plug-in electric vehicle aggregator in energy and reserve markets,” *Energy Convers. Manag.*, vol. 97, pp. 393–408, 2015.

[14] L. K. Panwar, K. S. Reddy, R. Kumar, B. K. Panigrahi, and S. Vyas, “Strategic Energy Management (SEM) in a micro grid with modern grid interactive electric vehicle,” *Energy Convers. Manag.*, vol. 106, pp. 41–52, 2015.

[15] Z. Hu, K. Zhan, H. Zhang, and Y. Song, “Pricing mechanisms design for guiding electric vehicle charging to fill load valley,” *Appl. Energy*, vol. 178, pp. 155–163, 2016.

[16] X. Dong, Y. Mu, X. Xu, H. Jia, J. Wu, X. Yu, and Y. Qi, “A charging pricing strategy of electric vehicle fast charging stations for the voltage control of electricity distribution networks,” *Appl. Energy*, vol. 225, no. 92, pp. 857–868, 2018.

[17] C. Jin, J. Tang, and P. Ghosh, “Optimizing electric vehicle charging: A customer’s perspective,” *IEEE Trans. Veh. Technol.*, vol. 62, no. 7, pp. 2919–2927, 2013.

[18] M. Ansari, A. T. Al-Awami, E. Sortomme, and M. A. Abido, “Coordinated bidding of ancillary services for vehicle-to-grid using fuzzy optimization,” *IEEE Trans. Smart Grid*, vol. 6, no. 1, pp. 261–270, 2015.

[19] Z. Xu, Z. Hu, Y. Song, W. Zhao, and Y. Zhang, “Coordination of PEVs charging across multiple aggregators,” *Appl. Energy*, vol. 136, pp. 582–589, 2014.

[20] M. Honarmand, A. Zakariazadeh, and S. Jadid, “Integrated scheduling of renewable generation and electric vehicles parking lot in a smart microgrid,” *Energy Convers. Manag.*, vol. 86, pp. 745–755, 2014.

[21] D. Thomas, O. Deblecker, and C. S. Ioakimidis, “Optimal operation of an energy management system for a grid-connected smart building considering photovoltaics’ uncertainty and stochastic electric vehicles’ driving schedule,” *Appl. Energy*, vol. 210, pp. 1188–1206, 2018.

[22] N. DeForest, J. S. MacDonald, and D. R. Black, “Day ahead optimization of an electric vehicle fleet providing ancillary services in the Los Angeles Air Force Base vehicle-to-grid demonstration,” *Appl. Energy*, vol. 210, pp. 987–1001, 2018.

[23] M. Shafie-khah, E. Heydarian-Forushani, M. E. H. Golshan, P. Siano, M. P. Moghaddam, M. K. Sheikh-El-Eslami, and J. P. S. Catalão, “Optimal trading of plug-in electric vehicle aggregation agents in a market environment for sustainability,” *Appl. Energy*, vol. 162, pp. 601–612, 2016.

[24] Y. Guo, J. Xiong, S. Xu, and W. Su, “Two-Stage Economic Operation of Microgrid-Like Electric Vehicle Parking Deck,” *IEEE Trans. Smart Grid*, vol. 7, no. 3, pp. 1703–1712, 2016.

[25] L. Yao, W. H. Lim, and T. S. Tsai, “A Real-Time Charging Scheme for Demand Response in Electric Vehicle Parking Station,” *IEEE Trans. Smart Grid*, vol. 8, no. 1, pp. 52–62, Jan. 2017.

[26] Q. Huang, Q. S. Jia, Z. Qiu, X. Guan, and G. Deconinck, “Matching EV Charging Load with Uncertain Wind: A Simulation-Based Policy Improvement Approach,” *IEEE Trans. Smart Grid*, vol. 6, no. 3, pp. 1425–1433, 2015.

[27] M. H. K. Tushar, C. Assi, M. Maier, and M. F. Uddin, “Smart microgrids: Optimal joint scheduling for electric vehicles and home appliances,” *IEEE Trans. Smart Grid*, vol. 5, no. 1, pp. 239–250, 2014.

[28] L. Jian, X. Zhu, Z. Shao, S. Niu, and C. C. Chan, "A scenario of vehicle-to-grid implementation and its double-layer optimal charging strategy for minimizing load variance within regional smart grids," *Energy Convers. Manag.*, vol. 78, pp. 508–517, 2014.

[29] L. Zhang, F. Jabbari, T. Brown, and S. Samuelsen, "Coordinating plug-in electric vehicle charging with electric grid: Valley filling and target load following," *J. Power Sources*, vol. 267, pp. 584–597, 2014.

[30] Y. Wu, A. Ravey, D. Chrenko, and A. Miraoui, "A Real Time Energy Management for EV Charging Station Integrated with Local Generations and Energy Storage System," in *2018 IEEE Transportation and Electrification Conference and Expo, ITEC 2018*, 2018.

[31] T. M. Hansen, R. Roche, S. Suryanarayanan, A. A. Maciejewski, and H. J. Siegel, "Heuristic Optimization for an Aggregator-Based Resource Allocation in the Smart Grid," *IEEE Trans. Smart Grid*, vol. 6, no. 4, pp. 1785–1794, 2015.

[32] N. Liu *et al.*, "A Heuristic Operation Strategy for Commercial Building Microgrids Containing EVs and PV System," *IEEE Trans. Ind. Electron.*, vol. 62, no. 4, pp. 2560–2570, 2015.

[33] L. Jian, Y. Zheng, and Z. Shao, "High efficient valley-filling strategy for centralized coordinated charging of large-scale electric vehicles," *Appl. Energy*, vol. 186, pp. 46–55, 2017.

[34] J. Yang, L. He, and S. Fu, "An improved PSO-based charging strategy of electric vehicles in electrical distribution grid," *Appl. Energy*, vol. 128, pp. 82–92, 2014.

[35] W. Su and M. Y. Chow, "Computational intelligence-based energy management for a large-scale PHEV/PEV enabled municipal parking deck," *Appl. Energy*, vol. 96, pp. 171–182, 2012.

[36] M. Ghofrani, A. Arabali, and M. Ghayekhloo, "Optimal charging/discharging of grid-enabled electric vehicles for predictability enhancement of PV generation," *Electr. Power Syst. Res.*, vol. 117, pp. 134–142, 2014.

[37] J. Tan and L. Wang, "Integration of plug-in hybrid electric vehicles into residential distribution grid based on two-layer intelligent optimization," *IEEE Trans. Smart Grid*, vol. 5, no. 4, pp. 1774–1784, 2014.

[38] W. Lausenhammer, D. Engel, and R. Green, "Utilizing capabilities of plug in electric vehicles with a new demand response optimization software framework: Okeanos," *Int. J. Electr. Power Energy Syst.*, vol. 75, pp. 1–7, 2016.

[39] B. Škugor and J. Deur, "Dynamic programming-based optimisation of charging an electric vehicle fleet system represented by an aggregate battery model," *Energy*, vol. 92, pp. 456–465, 2015.

[40] B. Škugor and J. Deur, "A bi-level optimisation framework for electric vehicle fleet charging management," *Appl. Energy*, vol. 184, pp. 1332–1342, 2016.

[41] W. B. Powell, J. J. Cochran, L. A. Cox, P. Keskinocak, J. P. Kharoufeh, and J. C. Smith, “Approximate Dynamic Programming I: Modeling,” *Wiley Encycl. Oper. Res. Manag. Sci.*, 2010.

[42] L. Zhang and Y. Li, “Optimal Management for Parking-Lot Electric Vehicle Charging by Two-Stage Approximate Dynamic Programming,” *IEEE Trans. Smart Grid*, vol. 8, no. 4, pp. 1722–1730, Jul. 2017.

[43] C. Keerthisinghe, G. Verbič, and A. C. Chapman, “Energy management of PV-storage systems: ADP approach with temporal difference learning,” *19th Power Syst. Comput. Conf. PSCC 2016*, pp. 1–7, 2016.

[44] H. Zhang, Z. Hu, Z. Xu, and Y. Song, “Optimal Planning of PEV Charging Station with Single Output Multiple Cables Charging Spots,” *IEEE Trans. Smart Grid*, vol. 8, no. 5, pp. 2119–2128, 2017.

[45] G. R. C. Mouli, P. Bauer, and M. Zeman, “Comparison of system architecture and converter topology for a solar powered electric vehicle charging station,” *9th Int. Conf. Power Electron. - ECCE Asia "Green World with Power Electron. ICPE 2015-ECCE Asia*, pp. 1908–1915, 2015.

[46] D. van der Meer, G. R. Chandra Mouli, G. Morales-Espana Mouli, L. R. Elizondo, and P. Bauer, “Energy Management System With PV Power Forecast to Optimally Charge EVs at the Workplace,” *IEEE Trans. Ind. Informatics*, vol. 14, no. 1, pp. 311–320, Jan. 2018.

[47] G. R. C. Mouli, M. Kefayati, R. Baldick, and P. Bauer, “Integrated PV Charging of EV Fleet Based on Energy Prices, V2G and Offer of Reserves,” *IEEE Trans. Smart Grid*, vol. 3053, no. c, pp. 1–1, 2017.

[48] S. K. Rahimian, S. C. Rayman, and R. E. White, “Maximizing the Life of a Lithium-Ion Cell by Optimization of Charging Rates,” *J. Electrochem. Soc.*, vol. 157, no. 12, p. A1302, 2010.

[49] S. K. Rahimian, S. Rayman, and R. E. White, “Optimal charge rates for a lithium ion cell,” *J. Power Sources*, vol. 196, no. 23, pp. 10297–10304, 2011.

[50] G. Sikha, P. Ramadass, B. S. Haran, R. E. White, and B. N. Popov, “Comparison of the capacity fade of Sony US 18650 cells charged with different protocols,” *J. Power Sources*, vol. 122, no. 1, pp. 67–76, 2003.

[51] K. Liu, K. Li, H. Ma, J. Zhang, and Q. Peng, “Multi-objective optimization of charging patterns for lithium-ion battery management,” *Energy Convers. Manag.*, vol. 159, no. January, pp. 151–162, 2018.

[52] K. Zhang, L. Xu, M. Ouyang, H. Wang, L. Lu, J. Li, and Z. Li, “Optimal decentralized valley-filling charging strategy for electric vehicles,” *Energy Convers. Manag.*, vol. 78, pp. 537–550, 2014.

[53] S. B. Peterson, J. Apt, and J. F. Whitacre, “Lithium-ion battery cell degradation resulting from realistic vehicle and vehicle-to-grid utilization,” *J. Power Sources*, vol. 195, no. 8, pp. 2385–2392, 2010.

[54] M. A. Hannan, M. M. Hoque, A. Hussain, Y. Yusof, and P. J. Ker, "State-of-the-Art and Energy Management System of Lithium-Ion Batteries in Electric Vehicle Applications: Issues and Recommendations," *IEEE Access*, vol. 6, pp. 19362–19378, 2018.

[55] L. Costa and P. Oliveira, "Evolutionary algorithms approach to the solution of mixed integer non-linear programming problems," *Comput. Chem. Eng.*, vol. 25, no. 2–3, pp. 257–266, 2001.

[56] M. S. Kuran, A. Carneiro Viana, L. Iannone, D. Kofman, G. Mermoud, and J. P. Vasseur, "A smart parking lot management system for scheduling the recharging of electric vehicles," *IEEE Trans. Smart Grid*, vol. 6, no. 6, pp. 2942–2953, 2015.

[57] W. B. Powell and S. Meisel, "Tutorial on Stochastic Optimization in Energy—Part II: An Energy Storage Illustration," *IEEE Trans. Power Syst.*, vol. 31, no. 2, pp. 1468–1475, Mar. 2016.

[58] "National Household Travel Survey," 2009. Available: http://nhts.ornl.gov

[59] Réseau de Transport D'électricité. Accessed on January 7, 2018. [Online].Available: http://clients.rte-france.com/index_en.jsp

[60] F. Ziel, "Forecasting Electricity Spot Prices Using Lasso: On Capturing the Autoregressive Intraday Structure," *IEEE Trans. Power Syst.*, vol. 31, no. 6, pp. 4977–4987, 2016.

[61] T. M. Hansen, E. K. P. Chong, S. Suryanarayanan, A. A. Maciejewski, and H. J. Siegel, "A partially observable markov decision process approach to residential home energy management," *IEEE Trans. Smart Grid*, vol. 9, no. 2, pp. 1271–1281, 2018.

[62] A. Schroeder and T. Traber, "The economics of fast charging infrastructure for electric vehicles," *Energy Policy*, vol. 43, pp. 136–144, 2012.

[63] C. Michelbacher, T. Stephens, A. Pesaran, D. Scoffield, M. Keyser, J. Zhang, S. Ahmed, A. Markel, C. Kreuzer, R. Hovsapian, I. Bloom, M. Shirk, E. J. Dufek, T. R. Tanim, R. Vijayagopal, J. Francfort, M. Mohanpurkar, A. Burnham, F. Dias, A. Meintz, A. N. Jansen, R. B. Carlson, and K. Hardy, "Enabling fast charging – Infrastructure and economic considerations," *J. Power Sources*, vol. 367, pp. 237–249, 2017.